Journal of Contaminant Hydrology 136–137 (2012) 86–95

Contents lists available at SciVerse ScienceDirect

Journal of Contaminant Hydrology

journal homepage: www.elsevier.com/locate/jconhyd

Impacts of bridging complexation on the transport of surface-modified nanoparticles in saturated sand

Saeed Torkzaban [a,*], Jiamin Wan [b], Tetsu K. Tokunaga [b], Scott A. Bradford [c]

[a] Commonwealth Scientific and Industrial Research Organisation (CSIRO) Land and Water, Private Bag 2, Glen Osmond, SA 5064, Australia
[b] Lawrence Berkeley National Laboratory, 1 Cyclotron Road, Berkeley, CA 94720, United States
[c] USDA, ARS, US Salinity Laboratory, Riverside, CA, United States

ARTICLE INFO

Article history:
Received 29 August 2011
Received in revised form 15 May 2012
Accepted 21 May 2012
Available online 28 May 2012

Keywords:
Nanoparticles
Transport
Deposition
Bridging complexation
DLVO theory

ABSTRACT

The transport of polyacrylic acid capped cadmium telluride (CdTe) quantum dots (QDs), carboxylate-modified latex (CML), and bare silica nanoparticles (NPs) was studied in packed columns at various electrolyte concentrations and cation types. The breakthrough curves (BTCs) of QDs and CML particles in acid-treated Accusand showed significant amounts of increasing deposition with 0.5, 1, and 2 mM Ca^{2+}, but only minute deposition at 50 and 100 mM Na^{+}. Negligible QD and CML deposition occurred at 2 mM Ca^{2+} in columns packed with ultrapure quartz sand that was similar in size to the Accusand. These observations are not consistent with interpretations based on Derjaguin–Landau–Verwey–Overbeek (DLVO) calculations of interaction energies. Scanning electron microscopy (SEM) and energy-dispersive X-ray (EDX) analysis demonstrated that there were regions on the acid-treated Accusand covered with small amounts of clay that were absent on the ultrapure quartz sand. A salt cleaning method was therefore used to remove the clay from the acid-treated Accusand. The BTCs of QDs and CML in this acid + salt treated Accusand exhibited much less deposition at any given Ca^{2+} concentration compared to those obtained from the acid-treated sand. SEM images showed that most of the QD deposited in acid-treated Accusand occurred on clay surfaces. Unlike our results with QDs and CML, negligible deposition of bare silica NPs occurred at 5 and 10 mM Ca^{2+} in acid-treated Accusand. The high deposition of QDs and CML particles was therefore attributed to bridging complexation in which Ca^{2+} serves as a bridge between the cation exchange locations on the clay and carboxyl functional groups on the QD and CML particles, which were absent on the bare silica NPs. Our results suggest that the transport of carboxylic ligand-modified NPs may be limited in subsurface environments because of the ubiquitous presence of clay and divalent cations.

1. Introduction

The fate and transport of engineered nanoparticles (NPs) in the subsurface environment are of particular interest for developing the best strategy of waste management and disposal of these materials. Engineered NPs may be either bare or surface-modified. A variety of surface-modifying agents such as carboxylic acid (e.g. polyacrylic and polyelectrolyte acid) and phosphorus containing acid (e.g. octylphosphonic acid, trioctylphosphine oxide) groups are used to modify the surface of engineered NPs (Kirby et al., 2004; Saleh et al., 2008). Research has shown that most of the bare NPs (e.g. hematite NPs, nC60, Nanotubes, nZVI, and $nTiO_2$) have a tendency to form large aggregates in aquatic systems and are less likely to travel long distances in the environment (Brant et al., 2005; Chen and Elimelech, 2006; Phenrat et al., 2008). This alleviates some of the concerns regarding potential adverse effects of these materials on both human health and aquatic environments. In contrast, surface-modified NPs have been shown to be more

* Corresponding author.
E-mail address: saeed.torkzaban@csiro.au (S. Torkzaban).

0169-7722/$ – see front matter © 2012 Elsevier B.V. All rights reserved.
doi:10.1016/j.jconhyd.2012.05.004

stable (i.e. resistant to aggregation) and mobile in aquatic environments (Phenrat et al., 2008; Saleh et al., 2007). Therefore, it is speculated that they may pose higher potential risks to the environment.

The stability and mobility of engineered NPs (either bare or surface-modified) in the subsurface are dependent on their particle–particle and particle–mineral interactions. The solution pH, ionic strength (IS), ion composition, and the surface coating of the NP will influence the interaction forces such as electrostatic, van der Waals, and steric forces (Phenrat et al., 2008). Research has shown that the stability and mobility of ligated NPs with polymers or surfactants are higher than that of bare NPs in deionized water and monovalent electrolytes (Saleh et al., 2007). However, these chemical conditions do not represent typical groundwater composition in which divalent cations, primarily Ca^{2+} and Mg^{2+}, are commonly present (Atekwana and Richardson, 2004). Some studies have addressed the effect of divalent cations on the stability and mobility of surface-modified NPs (Chen et al., 2006; Quevedo and Tufenkji, 2009; Saleh et al., 2008; Zhang et al., 2008). Chen et al. (2006) found that alginate-coated hematite exhibited significantly higher aggregation in $CaCl_2$ than in NaCl electrolyte. Zhang et al. (2008) demonstrated that the stability of thioglycolate-capped CdTe QDs was controlled by the solution ionic composition. Divalent and trivalent cations induced formation of QD aggregates, whereas QDs remained stable in the presence of monovalent electrolyte even at 150 mM. Saleh et al. (2008) systematically evaluated the effect of IS and cation type on the mobility of bare and surface-modified Nanoscale Zero Valent Iron (NZVI) in water-saturated silica sand columns. They found that the mobility of the surface-modified NZVI was higher than that of bare NZVI. However, the mobility of the surface-modified NZVIs was lower in the presence of divalent electrolyte (Ca^{2+}) compared with their mobility in the presence of monovalent electrolyte (Na^{+}).

Clays are ubiquitous minerals in all soil and aquifer sediments in both flocculated state and also as colloidal particles attached to the surface of sand grains (Roy and Dzombak, 1996; Sposito, 1984). Analysis of the so-called "clean" natural sands by scanning electron microscopy (SEM) equipped with an energy dispersive X-ray (EDX) has shown the presence of small amounts of clay minerals on sand grains (Bradford and Kim, 2010; Roy and Dzombak, 1996; Torkzaban et al., 2010). These clay particles are usually immobile during normal chemical and water flow conditions (Roy and Dzombak, 1996). On the surface of clay minerals, there are sites with charge imbalance from isomorphic substitution resulting in an excess negative charge (Sposito, 2008). As a result, multivalent cations (e.g. Ca^{2+}) may strongly bind to the negatively charged sites on the clay surface (Sposito, 2008). It is also known that the multivalent cations are strongly adsorbed to anionic groups, such as carboxylate or phenolate, on organic polymers (Greenland, 1971). Bridging complexation, or "cation bridging" (Greenland, 1971), occurs when anionic or polar functional groups (typically carboxylate-terminated molecules) become bound to a multivalent metal cation adsorbed by a negatively charged clay surface (Sposito, 2008). It has been shown that organic anions such as humic and fulvic acids are strongly adsorbed to clay particles in the presence of polyvalent cations (Greenland, 1971; Saini and MacLean, 1966). In a study by Janjaroen et al. (2010) a high deposition of *Cryptosporidium parvum* oocysts on Suwannee River Natural Organic Matter (SRNOM)-coated surfaces in Ca^{2+} electrolyte was observed even though DLVO theory (Derjaguin and Landau, 1941; Verwey and Overbeek, 1948) predicted a substantial energy barrier. The deposition was attributed to inner-sphere complexation of Ca^{2+} with carboxylic groups on both SRNOM and oocyst surfaces.

We expect that clay minerals in natural porous media (for example those on the surface of sand grains) are likely to have a significant effect on the subsurface mobility of surface-modified NPs through bridging complexation. In particular, we hypothesize that Ca^{2+} may interact with clays in natural porous media and acidic functional groups of NPs to cause high deposition and limited transport even in the presence of a sizeable energy barrier to attachment. However, most studies examining the transport and deposition of surface-modified NPs in natural porous media, which may contain clay, have been conducted in the presence of monovalent electrolyte (Petosa et al., 2010). The other studies that used divalent electrolyte either employed a porous media that lacked clay (Saleh et al., 2007) or used bare NPs in the transport experiments (Li et al., 2008; Wang et al., 2008). To the best of our knowledge, the study by Saleh et al. (2008) is the only one that examined the effect of cation type on the mobility of surface-modified NPs (i.e. NZVI) in sand columns. However, in this study the porous media was clean silica sand, which lacked clay particles.

The objective of this work was to examine the coupled effect of cation type and clay, present on the sand grains, on the transport and deposition of surface-modified NPs in saturated sand columns. The column experiments were conducted using three different sands (acid-treated Accusand, acid + salt treated Accusand, and ultrapure quartz sand) at different electrolyte concentrations and cation types. Three different types of NPs, namely functionalized (polyacrylic acid) quantum dots (QDs), carboxyl-modified latex (CML), and non-functionalized silica NPs, were used to evaluate the validity of our assumptions.

2. Material and methods

2.1. Preparation and characterization of the NPs

Water soluble polyacrylic acid capped CdTe QDs with diameters between 1 and 10 nm was supplied from Vive Nano Inc., Canada. Because CdTe solubility is very low in water (Moskowitz et al., 1994), the concentration of CdTe QDs in suspension was determined using ICP-MS (Perkin Elmer DRC II). The stock suspension of CdTe QDs with a concentration of 18 mM was diluted by a factor of 1000 resulting in a final concentration of about 1.44×10^{11} particles per ml. This value was calculated based on the average aggregate size of 45 nm of the QDs (determined by dynamic light scattering) and the CdTe density of 5.85 g/cm^3. Carboxyl-modified latex (CML) particles with a mean diameter of 200 nm and a concentration of ~5.68×10^{12} particles per ml were purchased from Polysciences, Inc. (Warrington, PA), and the stock suspension was diluted by a factor of 100. Silica nanoparticles (non-functionalized) with a

mean diameter of 100 nm and a concentration of ~9.55×10^{13} particles per ml were purchased from Polysciences, Inc. (Warrington, PA) and the stock suspension was diluted by a factor of 1000 for the experiments. It should be noted that the same dilution factors were chosen for aggregation and deposition experiments in order to obtain a similar final concentration of about 10^{11} particle/ml for each NP, and fresh suspensions were made for each experiment.

Analytical reagent-grade NaCl and $CaCl_2$ (Fisher Scientific) and deionized (DI) water were used to prepare electrolyte solutions with various concentrations (0.5–10 mM Ca^{2+} and 50 and 100 mM Na^+) buffered at pH 8 with 0.1 mM $NaHCO_3$ (Fisher Scientific). This pH = 8 was chosen in order to minimize NP aggregation and deposition in the sand columns. The electrophoretic mobility (EPM) of the NPs in each solution was measured using a ZetaPlus analyzer (Brookhaven Instruments Corp., Holtsville, NY). The zeta potential values were calculated using tabulated data provided by Ottewill and Shaw (1972). The hydrodynamic diameter of the NPs was assessed using dynamic light scattering (DLS) (Brookhaven Instruments Corp., Holtsville, NY).

2.2. Porous media

Accusand (Unimin Corporation, Le Sueur, MN) and ultrapure quartz sand (Charles B. Chrystal Co., Inc., NY) were used as the porous media for transport experiments. The physical and chemical characterization of Accusand is given by Schroth et al. (1996). Accusand was soaked in 70% HNO_3 for 16 h to remove metal oxides and organic materials. In order to raise the pH of the acid-washed sand to the normal level, the sand was thoroughly rinsed with DI water followed by five 20 min cycles of sonication in a water bath. Throughout this paper we refer to this sand as acid-treated Accusand. The average grain diameters of the Accusand and ultrapure quartz sand were 270 μm, with the diameter ranging from 250 to 300 μm.

Scanning electron microscopy (SEM) was used to study the general morphology of sand grains. The measurements were carried out with a Zeiss Gemini Ultra-55 Analytical Scanning Electron Microscope operating at 2 to 5 keV. To determine the elemental composition of the sand surface, an EDX spectroscopy detector was used together with the SEM. SEM and EDX analyses of the acid-treated Accusand showed that some regions of the sand surface were covered with trace amounts of kaolinite clay (Bradford and Kim, 2010; Torkzaban et al., 2010). The clay particles were largely removed from the grain surfaces of acid-treated Accusand using a cation exchange method described as follows. The sand was immersed in 0.5 M NaCl solution for 1 h in a sonication bath, then flushed with DI water, and finally sonicated in DI water for 1 h. These steps (i.e. soaking in NaCl solution, DI water flushing, and sonication) were repeated three times. After this cleaning treatment, the SEM images showed that a large portion of the clay particles were removed from the sand grains, and we refer to this sand as acid + salt treated Accusand in this paper. The detached clay particles were collected and their zeta potential was determined over a range of solution chemistries. Aqua regia acid was used to digest the surface of the acid-treated Accusand, the acid + salt treated Accusand, and the ultrapure quartz. The elemental concentrations of digested Fe, Al, Ca, and Mg were measured using ICP-MS.

2.3. Column studies

Transport and deposition of the NPs (QDs, latex, and silica) in the water-saturated columns packed with acid-treated Accusand, acid + salt treated Accusand, or ultrapure quartz sand were examined over a range of solution chemistries. The acrylic tube columns were 10 cm long, with inner diameters of 25 mm. The columns were wet-packed and the porosity was determined to be about 0.41 from analysis of breakthrough data of a conservative tracer ($NaNO_3$). The packed columns were first flushed with 5 pore volumes (PV) of DI water using a syringe pump followed with 5 PVs of electrolyte solution of interest. The chemical composition of the electrolyte was either Na^+ (50 and 100 mM) or Ca^{2+} (0.5–10 mM). Then, various pulses of the NP suspensions were introduced into the columns, followed by injection of 3 PVs of NP-free solution at the same flow rate and chemical composition. The superficial flow rate was 0.4 cm min^{-1} corresponding to an average pore-water velocity of 14 m/day and a column residence time (one pore volume) of 10.25 min. The total duration of each experiment was about 200 min. The column effluent was collected at a constant interval using a fraction collector and analyzed for the NP concentration using an UV/visible spectrometer or ICP-MS. The latter method was used to measure the Cd concentration of the QD suspensions. The transport experiments presented in this work were conducted in duplicate at each electrolyte concentration, and the results exhibited good reproducibility.

NPs have frequently been reported to be irreversibly retained in sand in a primary minimum interaction (Petosa et al., 2010). In this case, experimental determination of the deposition profiles for NPs is hampered by incomplete recovery of the deposited NPs from the sand. The amount of deposited NPs was therefore quantified by taking the difference between the total amount injected into the column and the numerically integrated amount in the effluent. The mass fraction of deposited NPs was subsequently determined as the ratio of the amount of deposited NPs to the total amount of injected NPs into the column. Additional information about the deposition profiles for NPs was inferred from simulations discussed below.

2.4. Mathematical model and analysis

The transport and deposition behavior of NPs (QDs and latex) in the water-saturated packed columns were simulated using the one-dimensional form of the advection–dispersion equation (ADE) that includes a term for irreversible, time-dependent deposition as:

$$\frac{\partial C}{\partial t}=\lambda v\frac{\partial^2 C}{\partial z^2}-v\frac{\partial C}{\partial z}-K_{dep}\psi_s C \tag{1}$$

where t is time (T; units of time), z is distance (L; units of length), C is the number of NPs in the aqueous phase (NL^{-3};

N is the NP number), λ is the dispersivity (L), v is the average pore water velocity (LT^{-1}), K_{dep} is the first-order deposition coefficient (T^{-1}), and ψ_s is a dimensionless Langmuirian blocking function that accounts for time-dependent deposition as (Adamczyk et al., 1994):

$$\psi_s = 1 - \frac{S}{S_{\max}} \tag{2}$$

where S is the concentration of deposited NPs in the sand (NM^{-1}; M denotes units of mass), and S_{max} is the maximum concentration of deposited NPs (NM^{-1}). The corresponding mass balance equation for deposited NPs is given as:

$$\rho_b \frac{\partial S}{\partial t} = \theta K_{dep} \psi_s C \tag{3}$$

where ρ_b is the soil bulk density (ML^{-3}) and θ is the volumetric water content (−).

The parameters K_{dep} and S_{max} depend on the solution and solid phase chemistry because of their influence on the adhesive interaction. In particular, the adhesive interaction energy that acts on the NPs near the solid water interface (SWI) increases with solution IS due to compression of the diffuse double layer thickness on homogeneous surfaces (Petosa et al., 2010), and increases the zone of influence associated with microscale charge variability on heterogeneous surfaces (Duffadar and Davis, 2008). All of these factors increase the number of NPs that interact with the SWI and thereby increases K_{dep}, and the fraction of the sand surfaces that is favorable for NP deposition (S_f) (Torkzaban et al., 2008). The value of S_{max} is proportional to the S_f (Bradford et al., 2009).

A modified version of the HYDRUS-1D code (Simunek et al., 2005) was used to numerically solve Eqs. (1)–(3). This code is coupled to a non-linear least square optimization routine based upon the Levenberg–Marquardt algorithm (Marquardt, 1963) to fit selected model parameters (K_{dep} and S_{max}) to the NP breakthrough curves (BTCs). The goodness of the model fit was assessed by calculation of the coefficient of linear regression (R^2) and the standard error coefficients of the optimized parameters. Other model parameters were experimentally measured (θ, ρ_b, v, and pulse duration) or determined from conservative solute ($NaNO_3$) tracer experiments ($\lambda = 0.1$ cm).

3. Results and discussion

3.1. Surface charge and particle size of nanoparticles

The values of electrophoretic mobility (EPM) of the NPs over the range of solution chemistries and IS used in the column experiments are given in Table 1. The zeta potentials were calculated from these EPMs and are presented in Table 2. As expected, the magnitude of the zeta potential for the NPs increased (less negative) with the concentration of Na^+ and Ca^{2+} due to compression of the electrostatic double layer (Elimelech et al., 1995). Increasing the Ca^{2+} concentration was more effective at decreasing the magnitude of the zeta potential than similar changes in the Na^+ concentration because of the dependency of charge screening on the ion valence (Quevedo and Tufenkji, 2009). Silica sand has been reported to have negatively charged zeta potentials under similar chemical conditions (Gregory, 2006). The zeta potential of clay particles originally deposited on the sand surface increased (less negative) with the Na^+ and Ca^{2+} concentration (Table 2). Therefore, the negative values of zeta potential of the NPs, silica sand, and clay may suggest unfavorable conditions for attachment.

Table 1
The average of measured values of electrophoretic mobility (EPM) for QDs, CML, and bare silica NPs in the indicated solution chemistries.

Solution chemistry	IS	EPM QDs	EPM CML	EPM silica
	mM		(μm/s)/(V/cm)	
50 mM NaCl	50	−2.26	−3.33	A
100 mM NaCl	100	−2.05	−2.83	A
0.5 mM $CaCl_2$	1.5	−2.12	−3.18	A
1 mM $CaCl_2$	3.0	−1.91	−2.76	A
2 mM $CaCl_2$	6.0	−1.63	−2.33	A
5 mM $CaCl_2$	15.0	a	a	−1.77
10 mM $CaCl_2$	30.0	a	a	−1.55

a — not measured (i.e., column experiment not conducted under given condition).

The average diameters of QDs, CML and bare silica NPs measured by DLS were 45, 190, and 100 nm in 100 mM Na^+ electrolyte, respectively. The NP suspensions showed very little aggregation over a period of 350 min. The stability of QDs in the presence of Na^+ was in general agreement with the behavior reported by Quevedo and Tufenkji (2009) and Zhang et al. (2008), where they observed that QDs remained stable (about 50 nm) in KCl electrolyte up to 150 mM. The average diameters of CML and bare silica NPs did not notably change during the time span of 350 min over the range of 0.5 to 5 mM Ca^{2+}. Similarly, it was observed that the size of QDs did not change much over the observation time of 350 min at low Ca^{2+} concentrations ($\leq$2 mM) (Fig. 1). Therefore, we may rule out the effect of particle aggregation on QD retention in our sand column experiments. It should be mentioned that Torkzaban et al. (2010) reported the average diameter of the QD particles in the stock solution measured with a transmission electron microscopy (TEM) to be 8 nm. The comparison of TEM and DLS data indicates that some of the QDs formed aggregates, even in the presence of Na^+. This

Table 2
The average and standard deviation (in parentheses) of measured zeta potentials for QDs (ζ_{QDs}), CML (ζ_{latex}), bare silica NPs (ζ_{silica}), and clay particles (ζ_{clay}) in the indicated solution chemistries.

Solution chemistry	ζ_{QDs}	ζ_{latex}	ζ_{silica}	ζ_{clay}
		mV		
50 mM NaCl	−40 (1.8)	−45 (4.1)	a	−42 (4.6)
100 mM NaCl	−30 (2.1)	−40 (3.8)	a	−30 (5.7)
0.5 mM $CaCl_2$	−60 (2.9)	−60 (4.2)	a	−43 (4.1)
1 mM $CaCl_2$	−50 (3.2)	−45 (2.8)	a	−38 (5.1)
2 mM $CaCl_2$	−30 (3.6)	−35 (3.6)	a	−34 (4.8)
5 mM $CaCl_2$	a	a	−30 (3.5)	−28 (6.2)
10 mM $CaCl_2$	a	a	−15 (2.7)	

a — not measured (i.e., column experiment not conducted under given condition).

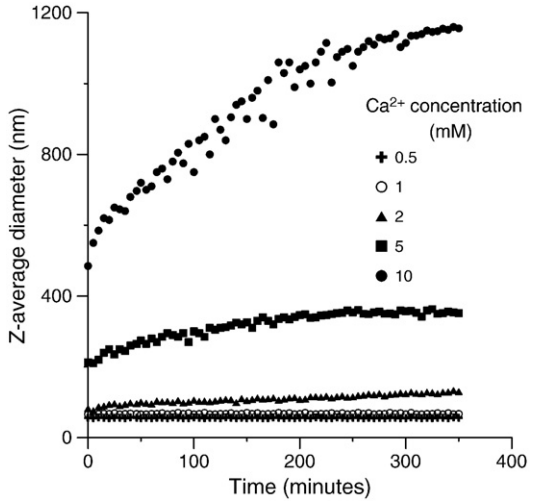

Fig. 1. Z-average diameters of the QDs obtained by DLS in different Ca^{2+} concentrations as a function of time. The QDs concentration was about 10^{11} particles per ml.

could be because of non-uniform coating of QD particles with polyacrylic acid ligands, and due to the thickness of the polymer coating and the surrounding electrical double layer. QD aggregation rates were high at 5 and 10 mM Ca^{2+}. At 10 mM Ca^{2+}, the Z-average diameters of the aggregates increased to more than 1 μm after 350 min (Fig. 1).

3.2. Transport experiments with CdTe quantum dots

Fig. 2 presents observed and simulated effluent BTCs for QDs in columns packed with acid-treated Accusand at 50 and 100 mM Na^+. Table 3 provides a summary of experimental and optimized parameters (K_{dep} and S_{max}) used in these simulations. After the QD breakthrough occurred, the normalized effluent concentrations rapidly reached one. Upon switching the influent to the QD-free solution, the effluent concentration sharply declined after one pore volume. These results indicate that the time required to saturate the available sites on the sand surface for deposition depended on the Na^+ concentration. Table 3 indicates that fitted $S_{max}^* = S_{max}/N_{ic}$ (where N_{ic} is the number of NPs in a unit volume of influent suspension) were equal to small values of 0.1 and 0.18 g^{-1} for 50 and 100 mM Na^+, respectively. The fitted values of K_{dep} were equal large values of 0.65 and 1.2 min^{-1} at 50 and 100 mM Na^+, respectively.

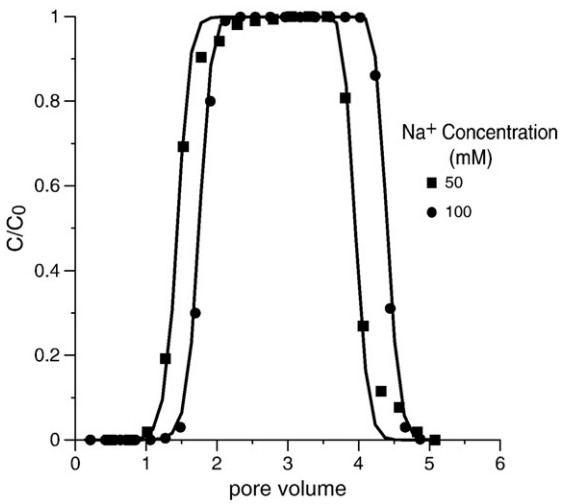

Fig. 2. Observed effluent concentration and corresponding model fits for QDs obtained from columns packed with acid-treated Accusand. Experiments were conducted at 50 and 100 mM Na^{2+}. Table 3 provides summary information on the model parameters.

Fig. 3a presents observed and simulated BTCs for QDs obtained from columns packed with acid-treated Accusand at 0.5, 1, and 2 mM Ca^{2+}. Model parameters are given in Table 3 and exhibited expected trends with increasing Ca^{2+} concentration (increasing K_{dep} and S_{max}). Table 4 shows that about 58%, 80%, and 96% of the injected QDs were deposited at 0.5, 1, and 2 mM Ca^{2+} concentration, respectively. The aggregation of QDs was minimal under these conditions (Fig. 1). The normalized effluent concentrations increased slowly with time, more pronounced at 0.5 and 1 mM Ca^{2+}. Detachment cannot account for this time-dependent deposition behavior because the BTCs exhibited negligible tailing. Conversely, the gradual filling (blocking) of the available sites for deposition was well described using a model that included Langmuirian blocking ($R^2 > 95\%$). This model predicts that the deposition profiles are initially exponential (log-linear) with depth (determined by K_{dep}), and then gradually approaches a uniform value of S_{max} as filling proceeds.

Comparison of the deposition behavior of QDs in the Ca^{2+} and Na^+ experiments indicates some interesting trends. In particular, QD deposition (Table 4) and S_{max}^* (Table 3) were much larger in the presence of Ca^{2+} than Na^+, even though the IS was much lower in the Ca^{2+} experiments (Table 1). Conversely, K_{dep} was much larger for Na^+ than for Ca^{2+} experiments (Table 3). These results demonstrate that the cation type and concentration had a significant effect on the transport and deposition of QDs in acid-treated Accusand.

At the first glance, it is tempting to attribute the underlying mechanisms causing the enhanced deposition of QDs in the presence of Ca^{2+} to surface charge reduction (e.g. higher compression of double layer thickness) and therefore increased attractive forces due to the divalent Ca^{2+}. DLVO theory is usually used to determine the interaction energies between colloids and mineral surfaces. These calculations are highly dependent on the Hamaker constant of the colloid–water–mineral surface (Jaisi and Elimelech, 2009). We were not able to determine a reliable value for the Hamaker constant of the QDs because they were capped with polyacrylic acid. This prevented us from determining the interaction energies between the QDs and sand. However, unfavorable conditions for deposition were expected as carboxyl groups on the surface of QDs have a pKa of 3.67 (Edsall and Wyman, 1958). Therefore, almost all of these functional groups are deprotonated at pH = 8 resulting in a negative surface charge to QDs. Moreover, DLVO calculations indicated the presence of a sizable repulsive energy barrier between CML particles and sand (to be discussed later in the paper). As a result, it is expected that the QDs should be repelled from negatively charged mineral surfaces such as the silica sand.

Table 3
Experimental conditions and fitted model parameters for column experiments shown in Figs. 2, 3, and 5.

NP	Cation mM	Sand cleaning	θ –	v m day^{-1}	λ cm	Pulse PV	K_{dep} min^{-1}	S^*_{max} g^{-1}	R^2 %
QD	Na = 50	Acid	0.41	14	0.1	3.0	0.65 (0.02)	0.10 (0.01)	98
QD	Na = 100	Acid	0.41	14	0.1	3.4	1.20 (0.05)	0.18 (0.02)	99
QD	Ca = 0.5	Acid	0.41	14	0.1	8.8	0.29 (0.01)	1.26 (0.02)	97
QD	Ca = 1.0	Acid	0.41	14	0.1	8.8	0.37 (0.03)	1.96 (0.05)	98
QD	Ca = 2.0	Acid	0.41	14	0.1	8.7	0.51 (0.04)	3.50 (0.07)	95
QD	Ca = 0.5	Acid + salt	0.41	14	0.1	8.8	0.12 (0.02)	0.33 (0.02)	99
QD	Ca = 1.0	Acid + salt	0.41	14	0.1	8.8	0.14 (0.01)	0.78 (0.03)	94
QD	Ca = 2.0	Acid + salt	0.41	14	0.1	8.7	0.23 (0.03)	1.28 (0.01)	96
CML	Ca = 0.5	Acid	0.41	14	0.1	8.8	0.31 (0.02)	1.74 (0.04)	97
CML	Ca = 1.0	Acid	0.41	14	0.1	8.8	0.46 (0.03)	2.40 (0.05)	99
CML	Ca = 2.0	Acid	0.41	14	0.1	8.7	0.81 (0.04)	3.90 (0.06)	98
CML	Ca = 0.5	Acid + salt	0.41	14	0.1	8.8	0.19 (0.01)	0.47 (0.02)	98
CML	Ca = 1.0	Acid + salt	0.41	14	0.1	8.8	0.22 (0.01)	0.94 (0.03)	99
CML	Ca = 2.0	Acid + salt	0.41	14	0.1	8.7	0.25 (0.01)	1.82 (0.05)	97

$S^*_{max} = S_{max}/N_{ic}$; where N_{ic} is the number of NPs in a unit volume of influent suspension.
Standard error values for the parameter fits are provided within the parentheses.

To better understand the role of cation type on QD deposition and to verify the existence of unfavorable conditions for attachment, an additional column experiment was conducted at 2 mM Ca^{2+} using ultrapure quartz sand as the porous media. In contrast to results from the acid-treated Accusand (Fig. 3a), the effluent concentration reached the influent concentration ($C/C_0 = 1$) after approximately one pore volume implying that QD deposition was negligible in the ultrapure quartz sand (≤1%) (data not shown). This result suggests that a significant energy barrier existed against attachment of the QDs to the ultrapure quartz sand. Ultrapure quartz sand has a similar grain size distribution, mineralogy, and surface charge as silica in the Accusand. Hence, differences in the deposition behavior for the ultrapure quartz sand and the Accusand cannot be explained by DLVO theory. The main difference between these two sands was in the natural weathering of the Accusand which resulted in the presence of trace amounts of clay on the sand grains. This weathering caused significant differences in the total amount of Fe, Al, Ca, and Mg for acid-treated Accusand (151 μg per g sand) and ultrapure quartz (2 μ g per g sand). Comparison of the QD deposition in acid-treated Accusand and ultrapure quartz sand therefore suggests that the significant amount of QD deposition in columns packed with Accusand in the presence of Ca^{2+} may be related to the existence of clay particles on the surface of Accusand grains.

Additional column experiments were conducted to investigate QD deposition in Accusand that was washed to remove

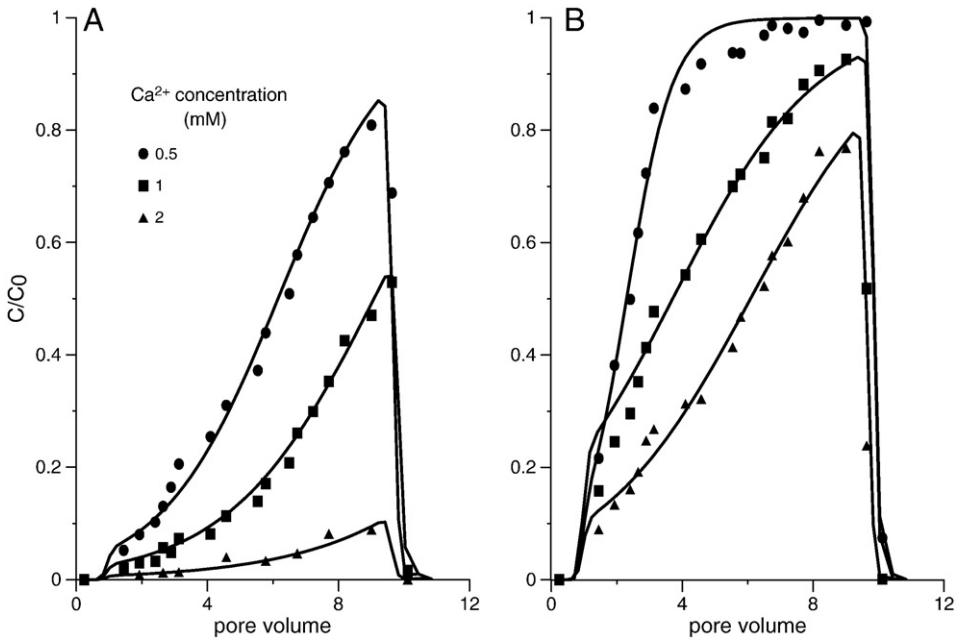

Fig. 3. Observed effluent concentration and corresponding model fits for QDs obtained from acid-treated (A) and acid + salt treated (B) Accusand at various Ca^{2+} concentrations. Table 3 provides information on the model parameters.

Table 4
The average and standard deviation (in parentheses) of mass deposition (%) for QDs, CML, and silica NPs in acid-treated and acid + salt treated Accusand at various Ca^{2+} concentrations.

Ca^{2+} (mM)	QDs		CML		Silica NPs
	Acid treated	Acid + salt treated	Acid treated	Acid + salt treated	Acid treated
0.5	54.8–62.7	20.7–11.9	74.5–70.1	25.5–21.1	a
1	82.7–77.1	34.6–39.6	91.1–88.2	46.2–42.9	a
2	96.1–96.6	55.6–59.7	99.2–99.5	72.5–70.8	a
5	a	a	a	A	1.9–3.6
10	a	a	a	A	6.1–5.2

a — not measured (i.e., column experiment not conducted under given condition).

the trace amounts of clay from the surfaces. Note that the Accusand used in both sets of experiments was acid-treated. The only difference was that the cation exchange method was used to remove the clay particles from the sand surfaces in the second series of experiments, referred to as acid + salt treated Accusand. SEM images of acid-treated and acid + salt treated Accusand showed that the majority of clay particles originally deposited on the sand surface were removed following the cation exchange treatment.

Observed and simulated BTCs for QDs obtained from the acid + salt treated Accusand exhibited a similar trend to the acid-treated Accusand (Fig. 3a), but much less deposition occurred on the acid + salt treated sand (Fig. 3b). The mass fraction of deposited QDs in acid + salt treated Accusand were about 16%, 37%, and 58% in 0.5, 1, and 2 mM Ca^{2+} concentration, respectively (Table 4). Values of K_{det} and S_{max}^{*} were also much lower for the acid + salt treated than the acid treated Accusand (Table 3) when the Ca^{2+} concentration was the same. The total amount of Fe, Al, Ca, and Mg recovered from acid + salt treated Accusand was equal to 44 μg per g sand, around one third the value for acid-treated Accusand. Comparison of the QD deposition in acid-treated and acid + salt treated Accusand therefore suggests that the deposition mainly occurred on the clay particles and locations associated with cation exchange.

To further explore the importance of clay on the deposition, a few grains of Accusand (acid-treated and acid + salt treated) were analyzed with SEM following the completion of the column experiments at 0.5 and 2 mM Ca^{2+}. The presence of deposited QDs on the sand was qualitatively determined in SEM images based on particle size and color, and comparison of SEM images before and after deposition experiments. We observed that most of the QDs were deposited on clay surfaces or in the locations where clay existed before removal by the cation exchange method (Fig. 4). Very few deposited QDs were detected on the smooth surfaces of sand grains suggesting the significant role of clay on the QD deposition. Moreover, no NP aggregates were observed on clay particles because the deposited QDs identified in the SEM images were about the same sizes as those measured by DLS.

3.3. Transport experiments with CML particles

The above information indicates that clay played a critical role in QD retention in the presence of Ca^{2+}. A similar series of column experiments was performed to assess the generality of these findings using CML particles. The BTCs for CML particles in the presence of 100 mM Na^{+} exhibited the same behavior (negligible deposition) as those of the QD experiments shown in Fig. 2 (data not shown). Fig. 5a and b presents observed and simulated BTCs for CML particles obtained from columns packed with acid-treated and acid + salt treated Accusand, respectively, at 0.5, 1, and 2 mM Ca^{2+}. Values of K_{det} and S_{max}^{*} were much lower on the acid + salt treated than the acid treated Accusand at similar Ca^{2+} concentrations (Table 3). Table 4 indicates that about 72%, 90%, and 99% of the CML particles were retained in the columns packed with acid-treated sand at 0.5, 1, 2 mM Ca^{2+} concentration, respectively. In contrast, only about 23%, 44%, and 72% of the CML particles were retained in columns packed with acid + salt treated sand at 0.5, 1, and 2 mM Ca^{2+} concentration, respectively. Comparison of model parameters and the amounts of CML deposition in acid-treated (Fig. 5a) and acid + salt treated (Fig. 5b) Accusand therefore suggests that the deposition mainly occurred on the clay particles. In addition, negligible CML retention ($\leq$1%) occurred in a column experiment packed with ultrapure quartz sand at 2 mM Ca^{2+}. DLVO calculations, using a Hamaker constant of 4.04×10^{-21} J (Bergendahl and Grasso, 1999), indicated the presence of a sizable repulsive energy barrier (>100 kT) and negligible secondary minimum at 2 mM Ca^{2+}. These observations are all consistent with the results obtained for QD, and further support the importance of clay and cation type on CML retention.

3.4. Bridging complexation

We hypothesize that bridging complexation was formed between anionic functional groups of QDs and CML and calcium cations adsorbed on the negatively charged clay minerals on the Accusand grains. As discussed in the Introduction, bridging complexation is an important reaction mechanism in which anionic functional groups (typically carboxylate-terminated molecules) become bound to a multivalent metal cation adsorbed by a negatively charged clay surface (Sposito, 2008). As a result, significant deposition of QDs and CML nanoparticles was observed even in the presence of a sizeable energy barrier predicted by DLVO theory. To test this hypothesis, we conducted additional deposition experiments using bare silica NPs in columns packed with the acid-treated Accusand in the presence of Ca^{2+}electrolyte (5 and 10 mM $CaCl_2$). Silica NPs do not have carboxyl functional groups like the QDs and CML particles, and bridging is therefore not expected to occur in this case. A negligible deposition for bare silica NPs was observed in these column experiments (Table 4), even though the zeta potential of bare silica NPs at 10 mM Ca^{2+} was almost the same as that of QDs at 2 mM Ca^{2+} (i.e., −20 mV).

In addition, deposition amount (Table 4) and S_{max}^{*} (Table 3) for CML particles was higher than QDs under similar conditions despite the fact that their zeta potentials were more negative than those of QDs. This result is likely due to the higher charge density of carboxylic groups on the surface of CML particles compared to QDs. In fact, this is in agreement with the lower zeta potential values of the CML particles compared to those of QDs (Table 2). Therefore, a higher density of carboxylic groups on CML particles interacting with the clay surface would

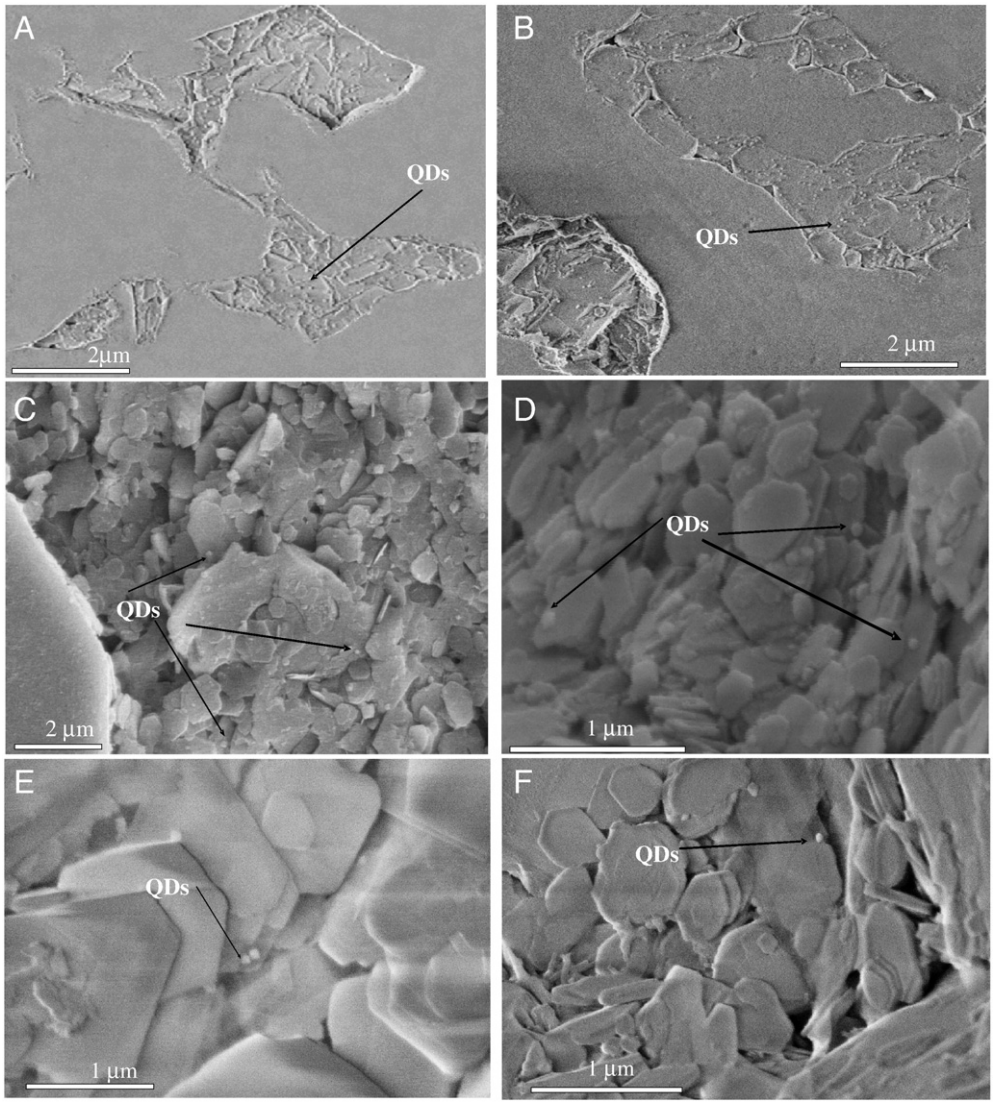

Fig. 4. SEM images showing that the QDs were mainly deposited on areas containing clay. QDs were deposited at 2 mM Ca^{2+} on acid + salt treated Accusand (A and B) and 0.5 mM Ca^{2+} acid-treated Accusand (C–F).

promote stronger adsorption by bridging complexation. Zhang et al. (2008) studied the stability of thioglycolate capped CdTe QDs in monovalent and polyvalent electrolytes. They observed that the QDs remained stable even at 150 mM KCl solution while aggregates occurred at relatively low concentrations ($\leq$2 meq/L) of divalent cation. It was concluded that multivalent cations may react with capping ligands of QDs to form complexes that bridge QDs inducing the formation of settable QD flocs. These results are consistent with our DLS results showing that at 5 and 10 mM Ca^{2+} the particle sizes increased significantly, while there was no increase in size at 100 mM Na^{+}. All of the above observations suggest that the organic ligands on the surfaces of QDs and CML particles and existence of clay on the Accusand grains caused the enhanced deposition of QDs and CML particles in the presence of Ca^{2+} due to bridging complexation.

Most of the reported transport studies for NPs have been conducted using a clay-free porous media like silica sand, monovalent electrolytes, and/or bare NPs (e.g. nC60, NZVI, and SWNTs) (e.g. Jaisi and Elimelech, 2009; Li et al., 2008; Petosa et al., 2010; Saleh et al., 2008; Wang et al., 2008). Surface modified NPs exhibit higher stability and mobility than bare NPs, and major differences in the deposition behavior of NPs were not observed in the presence of monovalent and divalent cations under these highly idealized conditions because bridging did not occur (Janjaroen et al., 2010). In contrast, results from this study indicate that the mobility of carboxylic ligand-modified NPs may be profoundly influenced by divalent cations and omnipresent clays in soil and aquifer sediments because of bridging. Hence, the reported mobility of modified NPs with ligands containing carboxylic groups in porous media lacking clay particles (e.g. silica sand) or in the presence of monovalent cations may be much higher than their transport potential in the natural environment. Here we did not study the effect of different NP surface modifiers and clays, but it is expected

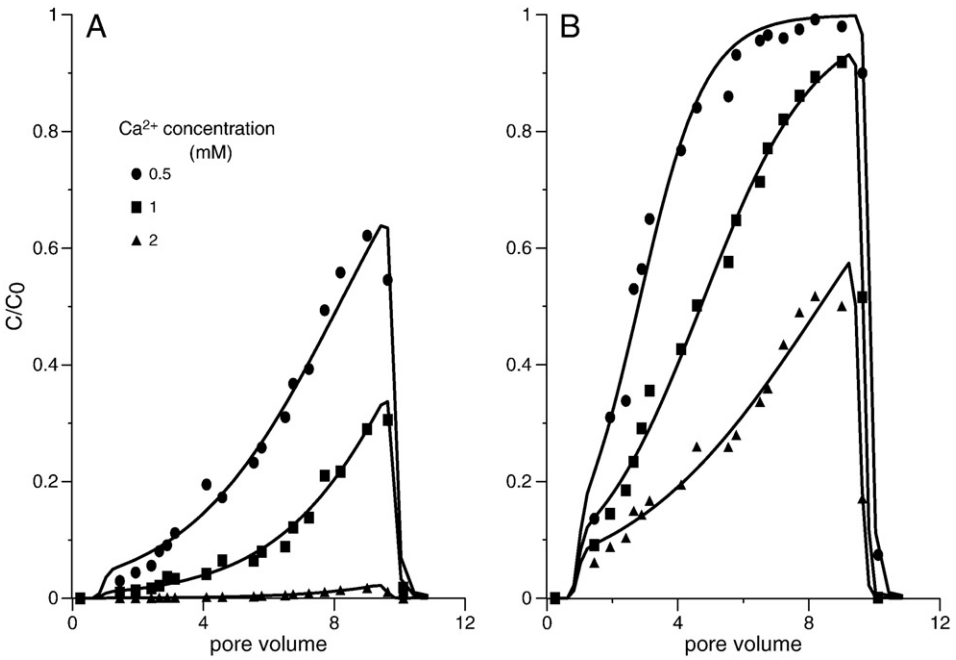

Fig. 5. Observed effluent concentration and corresponding model fits for CML particles obtained from acid-treated (A) and acid + salt treated (B) Accusand at various Ca^{2+} concentrations. Table 3 provides information on the model parameters.

that the different types of capping ligands and clays will also affect NP mobility in the subsurface. Nevertheless, interactions with clay particles and divalent cations are expected to be generally important in controlling transport of surface modified NPs.

Acknowledgments

Funding was provided through the joint BER-EPA-NSF Nanoparticulate Research Program of the Office of Biological and Environmental Research, U.S. Department of Energy, under contract DE-AC02-05CH11231. The authors are grateful to thoughtful comments and suggestions of Drs. Benjamin Gilbert and Yongman Kim from Lawrence Berkeley National Laboratory. Dr. Martin Mulvihill from the University of California, Berkeley is thanked for providing the SEM analyses. The authors would like to thank the anonymous reviewers for their valuable comments and suggestions to improve the paper.

References

Adamczyk, Z., Siwek, B., Zembala, M., Belouschek, P., 1994. Kinetics of localized adsorption of colloid particles. Advances in Colloid and Interface Science 48, 151–280.

Atekwana, E.A., Richardson, D.S., 2004. Geochemical and isotopic evidence of a groundwater source in the Corral Canyonmeadow complex central Nevada, USA. Hydrological Processes 18, 2801–2815.

Bergendahl, J., Grasso, D., 1999. Prediction of colloid detachment in a model porous media: thermodynamics. AIChE Journal 45, 475–484.

Bradford, S.A., Kim, H., 2010. Implications of cation exchange on clay release and colloid-facilitated transport in porous media. Journal of Environmental Quality 39, 1–7, http://dx.doi.org/10.2134/jeq2010.0156.

Bradford, S.A., Kim, H.N., Haznedaroglu, B.Z., Torkzaban, S., Walker, S.L., 2009. Coupled factors influencing concentration-dependent colloid transport and retention in saturated porous media. Environmental Science and Technology 43, 6996–7002.

Brant, J., Lecoanet, H., Wiesner, M.R., 2005. Aggregation and deposition characteristics of fullerene nanoparticles in aqueous systems. Journal of Nanoparticle Research 7 (4–5), 545–553.

Chen, K.L., Elimelech, M., 2006. Aggregation and deposition kinetics of fullerene (C60) nanoparticles. Langmuir 22 (26), 10994–11001.

Chen, K.L., Mylon, S.E., Elimelech, M., 2006. Aggregation kinetics of alginate-coated hematite nanoparticles in monovalent and divalent electrolytes. Environmental Science and Technology 40 (5), 1516–1523.

Derjaguin, B.V., Landau, L.D., 1941. Theory of the stability of strongly charged lyophobic sols and of the adhesion of strongly charged particles in solutions of electrolytes. Acta Physicochimica URSS 14, 733–762.

Duffadar, R.D., Davis, J.M., 2008. Dynamic adhesion behavior of micrometer-scale particles flowing over patchy surfaces with nanoscale electrostatic heterogeneity. Journal of Colloid and Interface Science 326, 18–27.

Edsall, J.T., Wyman, J., 1958. Biophysical Chemistry. Academic Press, New York.

Elimelech, M., Gregory, J., Jia, X., Williams, R.A., 1995. Particle deposition and aggregation: measurement. Modeling, and Simulation. Butterworth-Heinemann, Oxford.

Greenland, D.J., 1971. Interactions between humic and fulvic acids and clays. Soil Science 111, 34–41.

Gregory, J., 2006. Particles in Water: Properties and Processes. CRC Press, Taylor & Francis Group, London.

Jaisi, D.P., Elimelech, M., 2009. Single-walled carbon nanotubes exhibit limited transport in soil columns. Environmental Science and Technology 43 (24), 9161–9166.

Janjaroen, D., Liu, Y., Kuhlenschmidt, M.S., Kuhlenschmidt, T.B., Nguyen, T.H., 2010. Role of divalent cations on deposition of *Cryptosporidium parvum* oocysts on natural organic matter surfaces. Environmental Science and Technology 44 (12), 4519–4524.

Kirby, G.H., Harris, D.J., Li, Q., Lewis, J.A., 2004. Poly(acrylic acid)-poly(ethylene oxide) comb polymer effects on $BaTiO_3$ nanoparticle suspension stability. Journal of the American Ceramic Society 87 (2), 181–186.

Li, Y., Wang, Y., Pennell, K.D., Abriola, L.M., 2008. Investigation of the transport and deposition of fullerene (C60) nanoparticles in quartz sands under varying flow conditions. Environmental Science and Technology 42, 7174–7180.

Marquardt, D.W., 1963. An algorithm for least-squares estimation of non-linear parameters. Journal of the Society for Industrial and Applied Mathematics 11, 431–441.

Moskowitz, P.D., Steinberger, H., Thumm, W., 1994. Health and environmental hazards of CdTe photovoltaic module production, use and decommissioning. IEEE First World Conference on Photovoltaic Specialists Conference, pp. 115–118.

Ottewill, R.H., Shaw, J.N., 1972. Electrophoretic studies on polystyrene lattices. Journal of Electroanalytical Chemistry 37, 133–142.

Petosa, A.R., Jaisi, D.P., Quevedo, I.R., Elimelech, M., Tufenkji, N., 2010. Aggregation and deposition of engineered nanomaterials in aquatic environments: role of physicochemical interactions. Environmental Science and Technology 44, 6532–6549.

Phenrat, T., Saleh, N., Sirk, K., Kim, H.-J., Tilton, R.D., Lowry, G.V., 2008. Stabilization of aqueous nanoscale zerovalent iron dispersions by anionic polyelectrolytes: adsorbed anionic polyelectrolyte layer properties and their effect on aggregation and sedimentation. Journal of Nanoparticle Research 10 (5), 795–814.

Quevedo, I.R., Tufenkji, N., 2009. Influence of solution chemistry on the deposition and detachment kinetics of a CdTe quantum dot examined using a quartz crystal microbalance. Environmental Science and Technology 43, 3176–3182.

Roy, S.B., Dzombak, D.A., 1996. Colloid release and transport processes in natural and model porous media. Colloids and Surfaces 107, 245–261.

Saini, G.R., MacLean, A.A., 1966. Adsorption–flocculation reactions of soil polysaccharides with kaolinite. Soil Science Society of America Proceedings 30, 697–699.

Saleh, N., Sirk, K., Liu, Y., Phenrat, T., Dufour, B., Matyjaszewski, K., Tilton, R.D., Lowry, G.V., 2007. Surface modifications enhance nanoiron transport and NAPL targeting in saturated porous media. Environmental Engineering Science 24, 45–57.

Saleh, N., Kim, H.J., Phenrat, T., Matyjaszewski, K., Tilton, R.D., Lowry, G.V., 2008. Ionic strength and composition affect the mobility of surface-modified Fe^0 nanoparticles in watersaturated sand columns. Environmental Science and Technology 42 (9), 3349–3355.

Schroth, M.H., Ahearn, S.J., Selker, J.S., Istok, J.D., 1996. Characterization of Miller-similar silica sands for laboratory hydrologic studies. Soil Science Society of America Journal 60, 1331–1339.

Simunek, J., van Genuchten, M.Th., Sejna, M., 2005. The HYDRUS-1D software package for simulating the one-dimensional movement of water, heat, and multiple solutes in variably-saturated media—version 3.0, HYDRUS software series 1. Department of Environmental Sciences, University of California Riverside, Riverside, CA. 240 pp.

Sposito, G., 1984. The Surface Chemistry of Soils, 1st ed. Oxford University, New York.

Sposito, G., 2008. The Chemistry of Soils, 2nd Ed. Oxford University Press, New York.

Torkzaban, S., Tazehkand, S.S., Walker, S.L., Bradford, S.A., 2008. Transport and fate of bacteria in porous media: coupled effects of chemical conditions and pore space geometry. Water Resources Research 44, http://dx.doi.org/10.1029/2007WR006541 (Art. No. W04403).

Torkzaban, S., Kim, Y., Mulvihill, M., Wan, J., Tokunaga, T.K., 2010. Transport and deposition of functionalized CdTe nanoparticles in saturated porous media. Journal of Contaminant Hydrology 118, 208–217.

Verwey, E.J.W., Overbeek, J.Th.G., 1948. Theory of the Stability of Lyophobic Colloids. Elsevier, Amsterdam.

Wang, Y., Li, Y., Pennell, K.D., 2008. Influence of electrolyte species and concentration on the aggregation and transport of fullerene nanoparticles in quartz sands. Environmental Toxicology and Chemistry 27, 1860–1867.

Zhang, Y., Chen, Y., Westerhoff, P., Crittenden, J.C., 2008. Stability and removal of water soluble CdTe quantum dots in water. Environmental Science and Technology 42 (1), 321–325.